Amino Acids (2010) 39:899–910
DOI 10.1007/s00726-010-0524-4

SHORT COMMUNICATION

Acid-induced unfolding of didecameric keyhole limpet hemocyanin: detection and characterizations of decameric and tetrameric intermediate states

Ankita Varshney · Basir Ahmad · Gulam Rabbani · Vijay Kumar · Savita Yadav · Rizwan Hasan Khan

Received: 7 August 2009 / Accepted: 10 February 2010 / Published online: 7 March 2010

Abstract Keyhole limpet hemocyanin (KLH) is widely used as an immune stimulant and hapten carrier derived from a marine mollusc *Megathura crenulata*. To provide details of the stability and equilibrium of KLH, different intermediate species were investigated with a series of biophysical techniques: circular dichroism, binding of hydrophobic dye, 1-anilino-8-naphthalene sulfonic acid, acrylamide-induced fluorescence quenching, thermal stability and dynamic light scattering. KLH in its native state at pH 7.4 exists in the stable didecameric form with hydrodynamic radii (R_h) of 28.22 nm, which is approximately equal to a molecular mass of 8.8 ± 0.6 MDa. The experimental results demonstrated the presence of two structurally distinct species in the conformational transition of KLH under acidic conditions. One species populates at pH 2.8, characterized as decameric (4.8 ± 0.2 MDa; $R_h = 22.02$ nm), molten globule-like state, while the other accumulates at pH 1.2 and is characterized as a tetramer (2.4 ± 0.8 MDa; $R_h = 16.47$ nm) with more organized secondary and tertiary structures. Our experimental manipulation of the oligomeric states of KLH has provided data that correlate well with the known oligomeric forms obtained from total KLH formed in vivo and extends our understanding of multimer formation by KLH. The results are of particular interest in light of the important role of the mechanistic pathway of pH-dependent structural changes of Hc stability in the biochemical and medical applications of these respiratory proteins.

Keywords Acidic pH · Decamer state · Dynamic light scattering · Keyhole limpet hemocyanin · Multimeric protein · Tetramer state

Abbreviations

ANS	1-Anilino-8-naphthalenesulfonate
CD	Circular dichroism
DLS	Dynamic light scattering
Hc	Hemocyanin
KLH	Keyhole limpet hemocyanin
MG	Molten globule state
MRE	Mean residue ellipticity
PFC	Packed folded conformational state

Introduction

Interest in the molluscan hemocyanins is well established, based primarily on the unique immunostimulatory properties of keyhole limpet hemocyanin (KLH) from the marine mollusc *Megathura crenulata*. These extracellular biopolymers are oxygen carrier copper glycoproteins, forming freely dissolved aggregates in the hemolymph of molluscs with extremely high M_w (comparable in size to ribosomes or small viruses) and complex quaternary structure (Harris et al. 2000; Sterner and Decker 1994). They differ fundamentally from arthropod hemocyanins (Martin et al. 2007; Decker et al. 2007) and are extremely large proteins (6–7.5 million daltons) that occur either as decamers (five subunit dimers assembled as a hollow

A. Varshney · B. Ahmad · G. Rabbani · R. H. Khan (✉)
Interdisciplinary Biotechnology Unit, Aligarh Muslim University, Aligarh, UP 202002, India
e-mail: rizwanhkhan@hotmail.com; rizwanhkhan1@gmail.com

V. Kumar · S. Yadav
Department of Biophysics, All India Institute of Medical Sciences, Ansari Nagar, New Delhi 110029, India

cylinder), didecamers (face-to-face assembly of two decamers) or multidecamers (elongated cylinders formed from a didecamer with added decamers) (Harris and Markl 1999, 2000; Gatsogiannis and Markl 2009). Molluscan hemocyanins have been intensively studied for their structure, function and evolution, and for immunological and clinical applications (Van Holde et al. 1992; Van Holde and Miller 1995; Harris and Markl 1999). Several aspects of their structural–functional peculiarities make Hcs important materials to address relevant problems of structural biology, including molecular recognition among subunits, protein–water interactions or allosteric regulation (Dolashka-Angelova et al. 2007). Homogeneous decamer and didecamer structures consisting of only one kind of subunit are found in the bivalves of the genus *Yoldia*. In contrast, gastropod Hcs of *M. crenulata* (Gebauer et al. 1994), *Halotis tuberculata* (Lieb et al. 1999, 2001) and *Rapana thomasiana* (Gebauer et al. 1999a) display two distinct homodecameric forms, attributed to the presence of two different subunits, while *Concholepas concholepas* exhibits an unusual heterodecameric array of subunits (Ioannes et al. 2004). KLH consists of two immunologically, physicochemically, distinct Hc types, termed as KLH1 and KLH2 (Markl et al. 1991; Gebauer et al. 1994). These act as widely used immunological tool and promising tumor vaccine carriers (Kim et al. 2007; Sabbatini et al. 2007). Their protein structure and disassembly/reassembly behavior have been extensively studied (Orlova et al. 1997; Sohngen et al. 1997; Harris et al. 1998, 2000; Gebauer et al. 1999b, 2002; Mouche et al. 2003). The complete amino acid sequence of molluscan Hcs *H. tuberculata* (Keller et al. 1999; Lieb et al. 2000) and both KLH1 and KLH2 were found (Lieb and Markl 2004) and, recently, cryo EM/crystal structure hybrid model of KLH1 was created (Orlova et al. 1997; Gatsogiannis and Markl 2009). The field of cellular immunology has provided much relevant biomedical information on KLH and has led to the expansion of the use of KLH in experimental immunology and clinically as an immunotherapeutic agent, because KLH is equal, if not superior, to BCG and with far fewer side effects (Harris and Markl 1999; Riggs et al. 2002; Suminoe et al. 2008; Betting et al. 2009). While the immunological response to KLH has often been attributed to the carbohydrate moiety, rather than protein alone, the polypeptide chain of eight globular functional units constituting the elongated KLH subunit and the highly organized quaternary structure of the native molecule could create a scaffold on which multiple carbohydrate epitopes can be initially made available to the immune system. Optimal steric spacing of sugar residues could potentiate the observed potent stimulatory response, both in vivo and in vitro. It is predicted that these carbohydrate side chains project from the surface of KLH molecule as well as from the subunits, thereby providing immunogenicity (Geyer et al. 2005; Beck et al. 2007; Sandra et al. 2007; Dolashka-Angelova et al. 2009).

Profuse experimental studies, using different dissociation and reassociation conditions of the native mollusc Hc, e.g., removal of divalent cations (Bonafe et al. 1994; Sohngen et al. 1997; Dolashka-Angelova et al. 2003), pH changes and the addition of denaturing agents (Dolashka-Angelova et al. 2000), have helped to elucidate its subunit composition and structure (Van Holde and Miller 1995). As evident by the very low catalytic activity of molluscs, *Rapana* and Octopus Hcs, or arthropods, *Carcinus aestuarii* and *Limulus polyphemus* Hcs, the entrance to the active site is probably blocked by Leu or Phe residues, respectively (Hristova et al. 2008). The pH-dependent conformational transition was found to be responsible for the activation of functional units of Hcs, creating access to the active site for phenolic substances. There is a wealth of dissociation-reassembly data at neutral to high pH on KLH didecamers and dissociation intermediates (Gebauer et al. 1994; Sohngen et al. 1997; Dolashka-Angelova et al. 2003). Thus, we investigated the folding/unfolding of KLH and its oligomerization into the intermediate structures at low pH. Previously, molten globule states for several proteins under various denaturing conditions have been reported by us (Ahmad et al. 2005, 2006; Varshney et al. 2008) as well as by several other investigators (Paci et al. 2005; Greene et al. 2006; Yang et al. 2006; Gerber et al. 2007, 2008; Georgieva et al. 2008; Kather et al. 2008; Nishimura et al. 2008; Ramboarina and Redfield 2008; Cremades and Sancho 2008). We found that oligomerization of KLH didecamers quantitatively results in stable decameric and tetrameric forms not previously observed for KLH under such conditions. These two structurally distinct isoforms at pH 2.8 and 1.2 behave similarly at low pH. The results presented here led us to conclude that KLH has a usual homodecameric organization at pH 2.8 resembling the "molten globule state", which on further protonation results in a stable population of tetramers (composed of two-subunit dimers).

Materials and methods

Materials

Keyhole limpet hemocyanin, (lot no. H8283) and 1-anilino-8-naphthalene sulfonic acid were purchased from Sigma Chemical Co., USA. Guanidine hydrochloride (GnHCl) was obtained from Sisco Research Laboratories, India. All other reagents used in the study were of analytical grade.

Methods

Protein concentration was determined spectrophotometrically using $E^{1\%}_{1\ cm}$ of 2.10 at 280 nm (Lowry et al. 1951) on a Hitachi spectrophotometer, model U-1500.

pH-induced unfolding studies

Stock protein solution was prepared by exhaustive dialysis of hemocyanin against double distilled water. As much as 50 µl of protein stock solution was mixed with 1,950 µl of the following buffers: 20 mM sodium phosphate buffer (pH 7.4–5.8), 20 mM sodium acetate buffer (pH 5.4–3.6) and 20 mM glycine–HCl buffer (3.4–1.2). The final solution mixture was incubated for 4–6 h at room temperature before optical measurements.

Circular dichroism (CD) measurements

CD measurements were carried out with a Jasco spectropolarimeter, model J-720, equipped with a microcomputer. The instrument was calibrated with d-10-camphorsulfonic acid. All the CD measurements were made at 25°C with a thermostatically controlled cell holder attached to Neslab's RTE-110 water bath with an accuracy of ±0.1°C. Spectra were collected with a scan speed of 20 nm min^{-1} and response time of 1 s. Each spectrum was the average of four scans. Far UV-CD and near UV-CD spectra were taken at protein concentrations of 0.25 and 5 mg ml^{-1} with 0.1 and 1-cm path length cells, respectively. The results were expressed as mean residue ellipticity (MRE) in degree cm^2 $dmol^{-1}$, which is defined as:

$$\mathrm{MRE} = \theta_{\mathrm{obs}} \times \mathrm{MRW}/(10 \times 1 \times c) \quad (1)$$

where θ_{obs} is the CD in milli-degree, MRW the mean residual weight (115), l the path length of the cell and c the concentration of the protein. Helical content was calculated from the MRE values at 222 nm using the following equation as described by Chen et al. (1972):

$$\%\ \alpha\text{-helix} = [(\mathrm{MRE}_{222\mathrm{nm}} - 2,340)/30,300] \times 100. \quad (2)$$

Circular dichroism data were also analyzed by online available software, K2d (Andrade et al. 1993).

Fluorescence measurements

Fluorescence measurements were performed on Shimadzu spectrofluorimeter, model RF-540 equipped with a data recorder DR-3. The fluorescence spectra were measured at 25 ± 0.1°C with a 1-cm path length cell. The excitation and emission slits were set at 5 and 10 nm, respectively. Intrinsic fluorescence was measured by exciting the protein solution at 280 or 295 nm and emission spectra were recorded in the range of 300–400 nm. A stock solution of 1-anilino-8-naphthalene sulfonic acid (ANS) was prepared in distilled water and its concentration was determined using an extinction coefficient of $\varepsilon M = 5{,}000\ M^{-1}\ cm^{-1}$ at 350 nm. For ANS fluorescence in the ANS binding experiments, the excitation wavelength was set at 380 nm and the emission spectra were taken in the range of 400–600 nm.

Acrylamide quenching

In the quenching experiments, aliquots of 5-M quencher stock solution was added to a protein stock solution (5 mg/ml), which was further diluted ten times to a total solution of 3 ml to achieve the desired range of quencher concentration (0.1–1 M). The excitation wavelength was 295 nm and the emitted light intensity was integrated over the period of 1 s and detected at 300–400 nm. The results of the quenching reactions between the excited tryptophan side chains and acrylamide at corresponding $\lambda_{\max}$ were analyzed according to the (3) Stern–Volmer and (4) modified Stern–Volmer equation (Eftink and Ghiron1982):

$$F_0/F = 1 + K_{\mathrm{sv}}[Q] \quad (3)$$

$$F_0/(F_0 - F) = 1/(K_{\mathrm{c}}[Q]^{*}\mathrm{fa}) + 1/\mathrm{fa}. \quad (4)$$

where F_0 and F are the fluorescence intensities at an appropriate wavelength in the absence and presence of quencher, respectively, K_{sv} is the Stern–Volmer constant, fa the fraction of the tryptophans accessible to the quencher, K_{c} the collisional quenching constant, and Q the concentration of the quencher.

Thermal stability studies

To determine the thermal stability of the intermediate state relative to the native state, ellipticity changes at 222 nm were measured as a function of temperature. Protein solutions in 20 mM sodium phosphate buffer of pH 7.4, and 20 mM glycine–HCl buffer of pH 2.8 and pH 1.2 were thermostatically controlled using a NESLAB thermostat water bath model RTE-110. Samples were analyzed after 20 min of incubation at the desired temperature prior to the measurement to insure the attainment of thermal equilibration, and the temperature was continuously varied from 20° to 95°C at a constant rate of 5 ± 0.3°C. The melting temperature (T_{m}) values were calculated from the circular dichroism data.

Dynamic light scattering measurements

Dynamic light scattering measurements were done using RiNA laser spectroscatter 201 operating at wavelength 660 nm and illuminated by a 100-mW laser diode. The

purified and lyophilized samples used for the measurements were first dissolved in buffer solutions of the required pH values. The protein was dissolved in 20 mM of sodium phosphate buffer of pH 7.4, 20 mM of glycine–HCl buffer of pH 2.8 and 20 mM of glycine–HCl buffer of pH 1.2 for DLS measurements. The samples were degassed, spun down at 14,000 rpm for 10 min and filtered through 0.02-μM polyvinylidene difluoride filters (Millipore). The protein concentration used was 2 mg ml^{-1}. The samples were injected manually into the flow cell (30 μL). Data were acquired over 150 s, where each data point was averaged over 3 s at a sensitivity of 80%.

Results

To understand the correlation between folding and assembly of multimeric proteins, it is important to track the relation between local and global changes that affect the association/dissociation state of the protein. Hence, we present the conformational behaviors of whole hemocyanin molecules in acidic solutions. For this purpose, we used far UV-CD as a probe for secondary structure, multiple probes for tertiary structure, and DLS to probe its dissociation state. These approaches proved to be suitable tools for studying the Hc structure and conformational changes in solution. The sensitivity of these techniques allows studies to be performed using diluted protein solutions. In this way, problems connected with aggregation and low solubility of the giant keyhole limpet Hc could be avoided.

Far UV-circular dichroism

Changes in the secondary structure of hemocyanin (KLH) as a function of pH were followed by far UV-CD measurements in the region between 200 and 250 nm. Figure 1a shows the CD spectrum for the native hemocyanin (pH 7.4) possessing two minima, one at 208 and the other at 222 nm, which is the characteristic feature of α-helical protein (curve 1). The protein was found to contain approximately 14% α-helical structure, as calculated by methods of secondary structure determination (Chen et al. 1972; Andrade et al. 1993). The spectral features at pH 2.8 (curve 2) greatly resembled completely unfolded protein, but still possessed significant amount of CD signal compared to the 6-M GnHCl denatured protein. However, the protein at pH 1.2 (curve 3) showed similar features as that of the native state at pH 7.4 (curve 1). Acid-induced secondary structural changes of hemocyanin were also monitored by measurements of MRE at 222 nm (Fig. 1b) versus pH plots. The plot represents a set of smooth and partially "bell-shaped" curve with maxima between pH 2.6 and 3, without any sigmoid feature at extreme pH. The relative

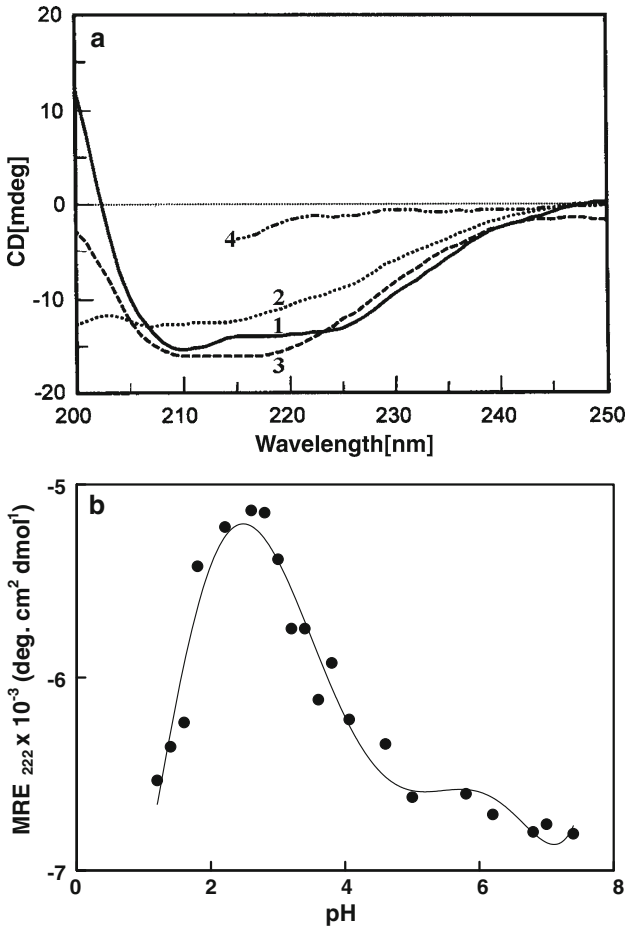

Fig. 1 **a** Far UV-CD spectra of hemocyanin: native protein at pH 7.4 (*curve 1*), molten globule state at pH 2.8 (*curve 2*), packed folded conformational state at pH 1.2 (*curve 3*) and 6-M GnHCl denatured state (*curve 4*). **b** Effect of pH on the mean residual ellipticity (MRE) of hemocyanin. Ellipticiity was monitored at 222 nm by far UV-CD. Protein concentration used was 0.25 mg/ml

changes were found to be small and almost noncooperative (in the vicinity of pH 2.8), indicating that acidic denaturation cannot be achieved as a reversible process for this intermediate species. But overall, the multimeric intact Hc had a small interval of partial reversibility under acidic conditions. Thus, it can be concluded that reversibility was possible in an acidic pH range, indicating the involvement of titrable groups responsible for structural stability. Previously, the effect of acidic and alkaline pH on dichroic spectra was monitored for RvH2-e (functional unit of *Rapana venosa* hemocyanin), but it was found to be pH independent due to the non-involvement of titrable groups (Dolashki et al. 2008; Velkova et al. 2009).

ANS fluorescence

Binding of ANS to the hydrophobic region of protein has been widely used to detect the molten globule state of

different proteins (Eftink and Ghiron 1982). Figure 2a shows the acid-induced unfolding of hemocyanin as monitored by ANS fluorescence at 480 nm. We observed minimum ANS fluorescence in the pH range 7.4–5.0. With decrease in pH, ANS intensity increased and was highest at pH 2.8. On further lowering of pH up to 1.2, significant decrease (about 50%) in the ANS fluorescence intensity was observed. But the ANS fluorescence at pH 1.2 was still high as compared to native and/or completely unfolded protein. Figure 2b shows the comparative emission fluorescence spectra in the 400–600 nm range. We observed blue shift in the λ_{max} of ANS fluorescence at pH 1.2 (480 nm) relative to native protein (498 nm) and protein at pH 2.8 (482 nm). This blue shifted fluorescence indicated burial of bound ANS due to the reorganization of protein secondary structure. Taken together, we may suggest that hemocyanin exists in the molten globule state (MG) at pH 2.8, which reorganizes into a packed folded-like conformational state (N^*) at pH 1.2.

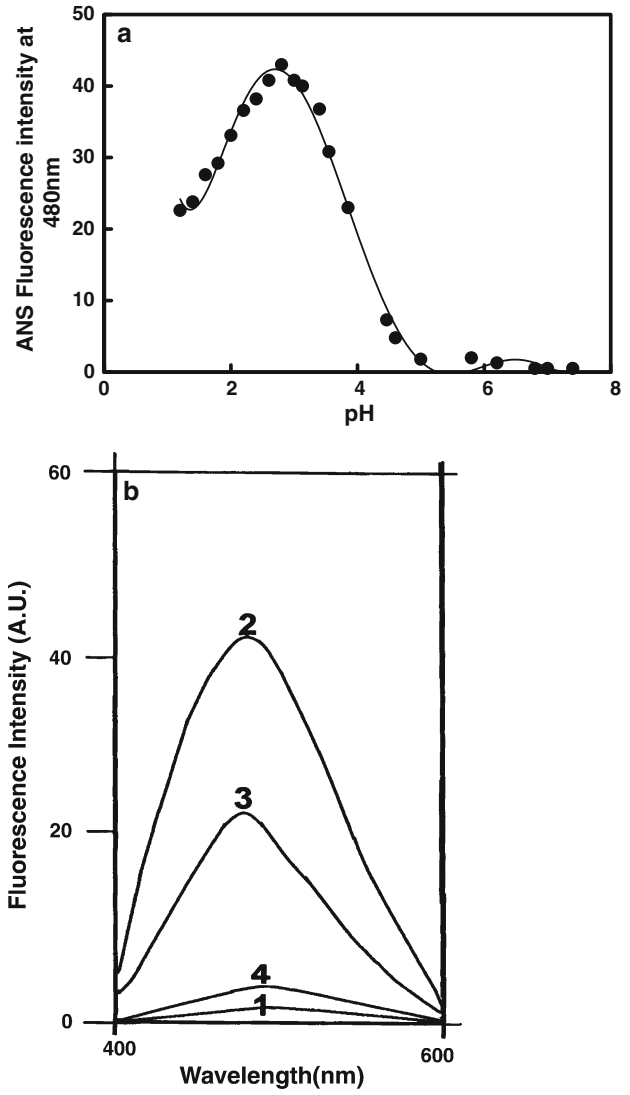

Fig. 2 **a** ANS fluorescence of hemocyanin as a function of pH. **b** Fluorescence emission spectra of ANS bound to native protein at pH 7.4 (*curve 1*), molten globule state at pH 2.8 (*curve 2*), packed folded conformational state at pH 1.2 (*curve 3*) and completely denatured protein in 6-M GnHCl (*curve 4*)

Intrinsic tryptophan fluorescence

The spectral features of tryptophanyl fluorescence (λ_{max} and intensity) are dependent on the dynamic and electronic properties of the chromophore environment; hence, steady state tryptophan fluorescence has been extensively used to obtain information on the structural changes of the protein (Semisotnov et al. 1991; Ahmad et al. 2005). The alterations of microenvironment of tryptophan residues of KLH have been monitored by studying the changes in the intensity and λ_{max} of tryptophanyl fluorescence as a function of pH (Fig. 3, Table 1). The fluorescence intensity at 340 nm and λ_{max} showed no apparent change between pH

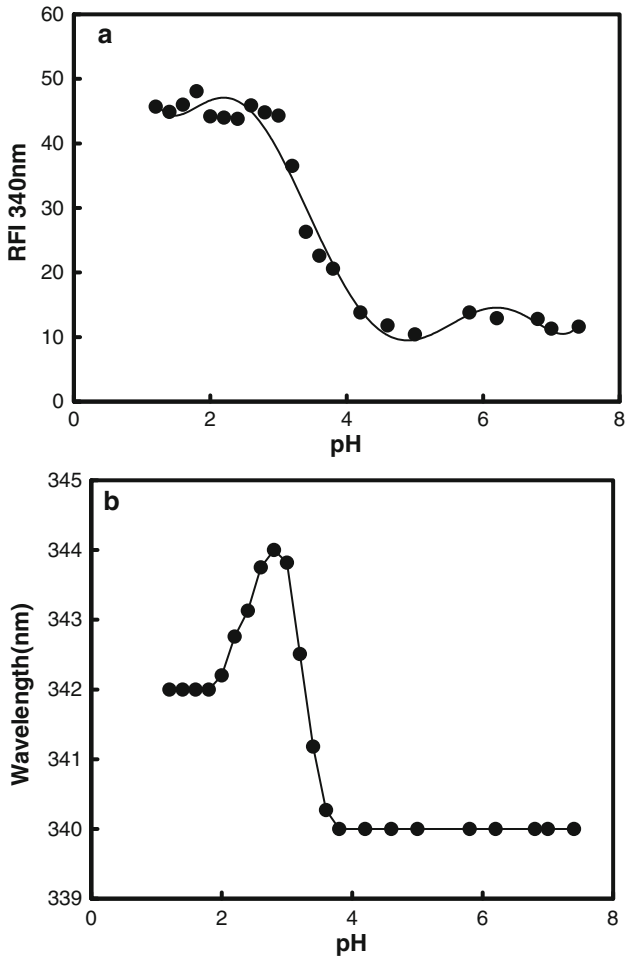

Fig. 3 **a** Tryptophan fluorescence: relative fluorescence intensity of tryptophan residues at 340 nm in hemocyanin as a function of pH, $\lambda_{ex} = 295$ nm. **b** Change in the emission wavelength maximum (λ_{max}) as function of pH, $\lambda_{ex} = 295$ nm

Table 1 Summary of different spectral properties of keyhole limpet hemocyanin

Variable	Native state (pH 7.4)	Molten globule state (pH 2.8)	Packed folded conformational state (pH 1.2)	GnHCl denatured state (6 M)
MRE_{222} nm[a]	−6,502	−5,146	−6,533	−590
% α-Helix[a1]	13	9.2	14	–
% α-Helix[a2]	14	8.6	16	–
Ext. 280nm[b]				
RFI_{340} nm	100	386	393	518
λ_{max}	331	340	331	348
Ext. 295nm[b]				
RFI_{340} nm	100	244	137	348
λ_{max}	332	344	334	356
Ext. 380 nm				
RFI_{480} nm	0.5	43	22.6	0.8
λ_{max}	498	482	480	502
Near UV-CD				
Shoulders (nm)	290 and 281	271 and 287	267, 278 and 296	261 and 279
Minima (nm)	269, 285 and 296	268 and 292	272, 283 and 287	275 and 283
Thermal transition[c]				
Cooperativity	Cooperative	Non-cooperative	Cooperative	–
T_m value	80°C	75°C	79°C	–

[a] MRE = degree cm^2 $dmol^{-1}$ (%α-helical content determination: [a1] Method of Chen et al. [a2] Online K2d Software)

[b] Fluorescence of native protein was taken as 100%

[c] As measured by MRE_{222} nm values

7.4 and 4.0, and when pH decreased below 4.0 up to 2.8, fluorescence intensity increased markedly with a red shift. On further lowering of pH up to 1.2, no apparent change was observed in fluorescence intensity, while λ_{max} was blue shifted. Figure 4a and b shows the intrinsic fluorescence emission spectra of KLH at pH 7.4 (native state), pH 2.8 (molten globule state), pH 1.2 (packed folded conformational state) and in the presence of 6-M GnHCl when protein was excited at 280 nm (where phenol and indole groups absorb) and 295 nm (exciting only trptophyl side chains), respectively. A red shift of 4 nm in the pH range 7.4–2.8 indicated that the microenvironment of tryptophanyl residue was getting more polar. This increase in fluorescence intensity during unfolding of the protein under acidic conditions might be due to relief in quenching of some tryptophanyl residues. It can be concluded that on excitation of the hemocyanin at 295 and 280 nm, the fluorescence emission of tryptophyl residues get "buried' deeply in the hydrophobic interior of the protein globules, suggesting transition of some indole rings from a hydrophobic to a more polar environment that occurs on dissociation of the hemocyanin aggregates. We observed changes in the emission maxima of KLH more abruptly at 295 nm, varying from 332 to 344 nm. Previously, similar results have been reported for KLH1 subunit of Hc with

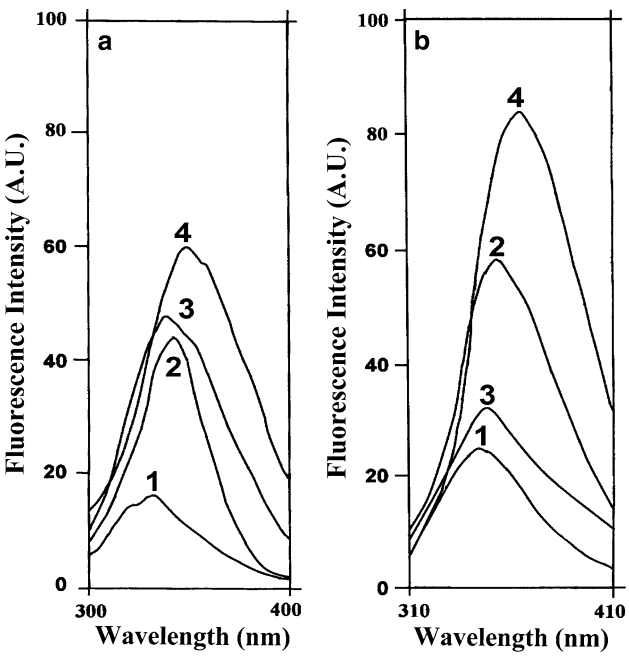

Fig. 4 Fluorescence emission spectra of hemocyanin when protein was excited at **a** 280 nm and **b** 295 nm. Hemocyanin in the native state at pH 7.4 (*curve 1*), molten globule state at pH 2.8 (*curve 2*), packed folded conformational state at pH 1.2 (*curve 3*) and in the presence of 6-M GnHCl (*curve 4*)

λ_{max} values of 336–340 nm, while for KLH2 it ranges from 335 to 336 nm. The same effect was observed for didecameric oxy-Hc of *R. thomasiana* groose molecule and its subunits (Dolashka et al. 1996). Furthermore, shift in the emission maxima at 295 nm depicts that Trp residues might be located in the vicinity of the active site of KLH functional unit. The partial unfolding of the KLH in these pH regions was also supported by far UV-CD, further indicating loss of secondary structure. This finding was further supported by quenching studies with a neutral quencher acrylamide.

Acrylamide quenching studies

The fluorescence properties of Trp residues can be used to obtain topological information of proteins. Fluorescence quenching of the tryptophanyl residues by neutral quencher (acrylamide) has been shown to be useful to obtain information about the solvent accessibility of these residues in proteins and the polarity of their microenvironment, as it can discriminate between 'buried' and 'exposed' side chains (Pawar and Deshpande 2000). Its ability to collosionally quench the excited indole rings depends only on their 'exposure' to the quencher. Figure 5a and b depicts the Stern–Volmer and modified Stern–Volmer plots for the acrylamide quenching studies performed on the native, MG, N^* and unfolded (6-M GnHCl) states. The values of Stern–Volmer constant (K_{sv}) and fractional accessibility of Trp residues to quencher (fa) were calculated from the above plots and presented in Table 2. The observed linearity of the plots can be explained by the similarity of the individual K_{sv} constants. It was interesting to note that K_{sv} for MG state ($K_{sv} = 5.2$) was found to be markedly higher compared to the N state ($K_{sv} = 0.70$) and was accompanied by a red shift in λ_{max} from 340 to 344 nm of Trp, supported by increase of fa from 0.47 to 1 on decrease of pH from 7.4 to 2.8. The acrylamide quenching efficiency for the native Hc ($K_{sv} = 0.70\ M^{-1}$) was very low compared to $K_{sv} = 16.33\ M^{-1}$ of tryptophan in aqueous solution. These results indicated that Trp residues in MG state were highly accessible to the quencher. In the presence of 6-M GnHCl wherein protein was considered to exist in a random coil conformation, we found K_{sv} and fa (11.52 and 1.13) to be much higher than the acid unfolded state. These results together with intrinsic fluorescence indicated that N^* state at pH 1.2 possesses Trp residues microenvironment, closely resembling that of native protein (Eftink and Ghiron 1982; Ahmad et al. 2005). As shown in Table 2, fractional accessibility of the acrylamide to the Trp residues of KLH follows the order:

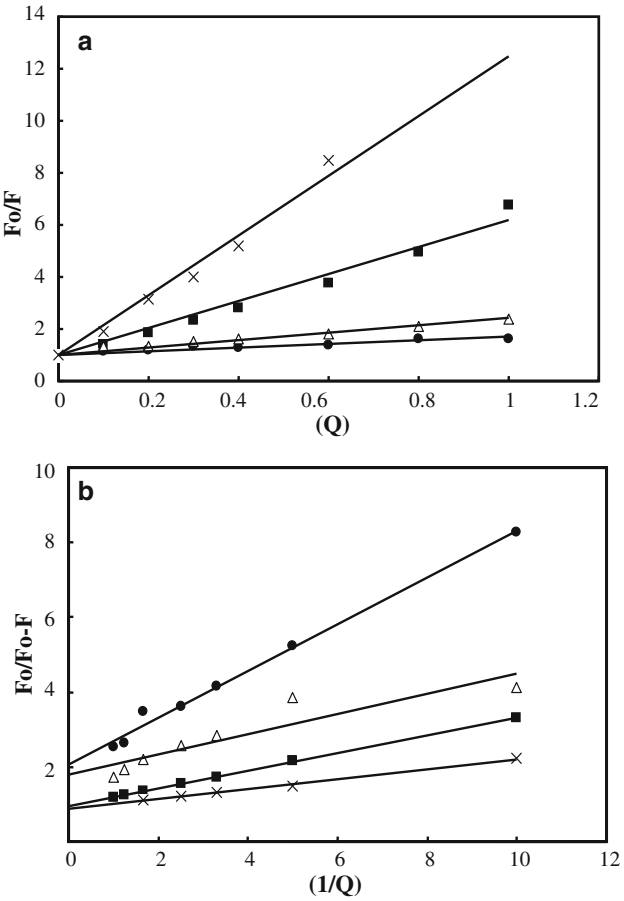

Fig. 5 Acrylamide quenching: Stern–Volmer **a** and modified Stern–Volmer **b** plots for hemocyanin at native pH 7.4 (*filled circles*), molten globule state at pH 2.8 (*filled squares*), packed folded conformational state at pH 1.2 (*open triangles*) and 6-M GnHCl state (*multiple symbols*)

Table 2 Fluorescence parameters (K_{SV} and fa) for acrylamide quenching of keyhole limpet hemocyanin

pH	K_{sv} (M^{-1})	fa (%)
7.4	0.7017	0.4766
2.8	5.1913	1.0463
1.2	1.4217	0.5575
6-M GnHCl	11.511	1.1273

$$U > MG(pH\,2.8) > N^*(pH\,1.2) > N.$$

This also indicates the comparative compactness of these intermediate states.

Near UV-circular dichroism

To study the tertiary structural alterations in more detail, CD measurements in the near UV region were performed at pH 7.4, 2.8, 1.2 and in the presence of 6-M GnHCl (Fig. 6a). Near UV-CD spectra of native KLH (pH 7.4)

shows two maxima at 290 and 281 nm and three minima at 296, 285 and 269 nm (Table 1). This indicates that the main contribution to the near UV-CD spectrum of native KLH was due to the Trp and Tyr residues. In the molten globule state at pH 2.8, there was an increase in signal and loss of fine structure, which are present in native protein. The near UV-CD spectrum of molten globule state resembled greatly the GnHCl denatured protein, although it retained a significant amount of signal compared to the GnHCl unfolded protein. At pH 1.2, regain in the ellipticity was observed and the protein at pH 1.2 showed almost an equivalent amount of tertiary structure compared to native KLH. Characteristic near UV-CD features of native KLH as mentioned above were not observed, suggesting that the tertiary structure formed in *N** state was non-native.

Thermal stability studies

Thermostability and stability is an important property of biomolecules, especially regarding their practical application. Figure 6b showed the temperature-induced conformational stability of KLH against heat at pH 7.4, 2.8 and 1.2 by following the changes in MRE measurements at 222 nm. As can be seen from Fig. 6b, temperature-induced unfolding transitions of native and *N** states are cooperative and weakly cooperative processes, as they are characterized by well-defined post- and pre-transition regions. Temperature-induced unfolding of KLH at pH 2.8 showed gradual increase in MRE at 222 nm, indicating continuous loss in the secondary structure content in the temperature range 20–95°C. This result shows that unfolding of molten globule state is non-cooperative. Similar temperature-induced unfolding behaviors of KLH at pH 7.4 and 1.2 could be explained on the basis of ordered secondary structure of these state. On the other hand, non-cooperative unfolding of KLH at pH 2.8 may be due to unfolded secondary structure as described in the far UV-CD section. Thus, the thermal-induced unfolding of KLH was found to be irreversible in nature. Probably, this is a common problem for the giant Hc molecules; the heat denaturation of the arthropodan Hc from *Palinurus vulgaris* and gastropod *R. thomasiana* were also found to be irreversible (Guzman-Casado et al. 1990; Dolashka et al. 1996). The T_m values were determined as midpoints of the transition curves. The native and packed folded conformational states of Hc have almost similar T_m (Table 1). Evidently, the molten globule state of Hc is considerably more stable than the native and packed folded conformational state.

Phase diagram method

The traditional approach to verify the accumulation of an intermediate state during the protein unfolding or refolding was to compare the unfolding curves detected by different

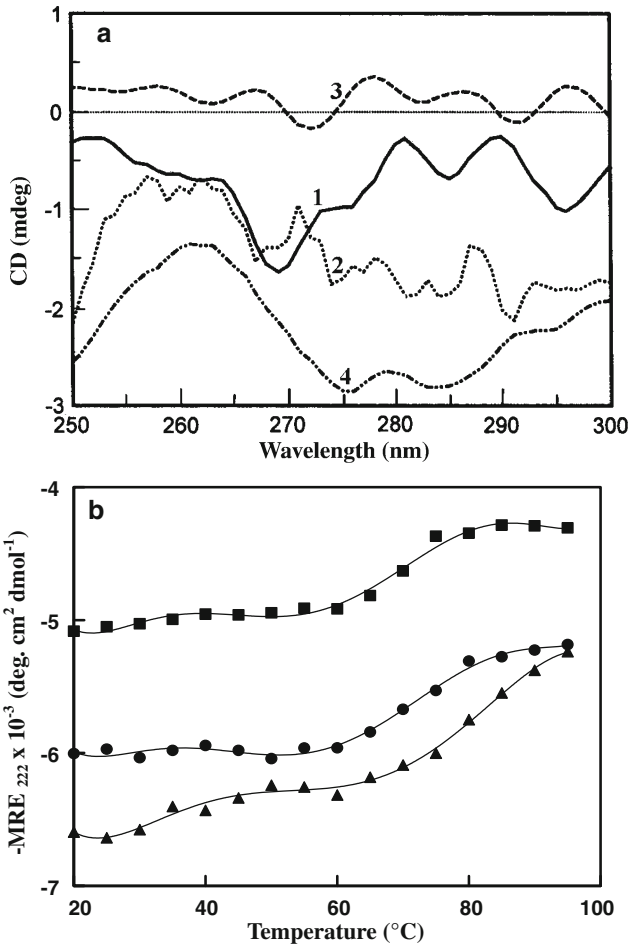

Fig. 6 **a** Near UV-CD spectra of hemocyanin in the native state (*curve 1*), molten globule state at pH 2.8 (*curve 2*), packed folded conformational state at pH 1.2 (*curve 3*) and completely denatured state in 6-M GnHCl state (*curve 4*). Spectra were recorded in the wavelength region 250–300 nm. Protein concentration used was 0.5 mg/ml. **b** Temperature dependence of CD spectrum of hemocyanin. Native state at pH 7.4 (*filled circles*), molten globule state at pH 2.8 (*filled squares*), packed folded conformational state at pH 1.2 (*open triangles*). Experiments were carried out in the temperature range 20–95°C

biophysical methods sensitive to the different structural levels of a protein molecule. The noncoincidence of such curves is considered as an argument in favor of the intermediate state of accumulation (Kuznetsova et al. 2003). Figure 7a represents a phase diagram for the pH-induced conformational changes induced in KLH. This diagram being plotted as dependence of fluorescence intensity at 340 nm on MRE_{222nm}, possesses two linear parts, i.e., it indicates the existence of two subsequent transitions $N \rightarrow MG \rightarrow N^*$ during oligomerization of KLH at low pH.

Dynamic light scattering

Two different hemocyanin isoforms, KLH1 and KLH2, have been found in the hemolymph of the keyhole limpet

M. crenulata with molecular masses of ~8 MDa, such that native didecamers yielded a mass difference of about 800 kDa between KLH 1 and KLH 2 (8.3 vs. 7.5 MDa) (Hartmann et al. 2004; Sohngen et al. 1997). KLH displays different oligomeric states and stabilities. At pH 7.4, KLH exists as didecamer and shows hydrodynamic radii of 28.22 nm, approximately equal to a molecular mass of 8.8 ± 0.6 MDa, and is stable (Fig. 7b). KLH didecamer dissociates to decamer (4.8 ± 0.2 MDa; hydrodynamic radii of 22.02 nm) at pH 2.8. On further lowering of pH to 1.2, it dissociates to a tetramer (2.4 ± 0.8 MDa) corresponding to a hydrodynamic radius of 16.47 nm. Thus, we conclude that KLH exists primarily in the multimeric state and dissociates to the decameric state that possesses characteristics of a molten globule, which, on further lowering the pH to 1.2, forms a tetramer. These tetramers might form due to dimerization of dimers as reported previously (Orlova et al. 1997). These dimers could be defined as packed folded-like conformational state, as they regain the structure similar to that of native Hc KLH.

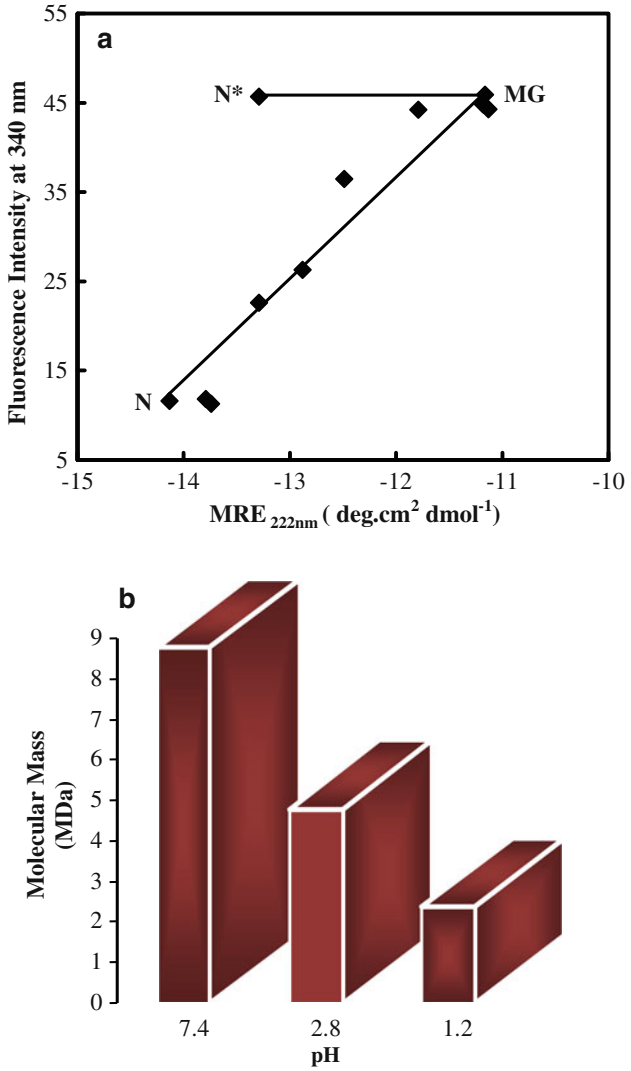

Fig. 7 **a** Phase diagram representation [fluorescence intensity at 340 nm vs. MRE $_{222nm}$ (degree cm^2 dmol^{-1})] of the pH-induced conformational changes in KLH. **b** Measurement of molecular dimension and hydrodynamic radii of KLH at different pH (7.4, 2.8 and 1.2)

Discussion

At present, there is a growing interest in hemocyanins; from a scientific viewpoint, this attention is focused on their structure, evolution and diversity (Van Holde et al. 1992; Van Holde and Miller 1995), whereas from the biomedical viewpoint, it concerns the relationship among their structural features and immunotherapeutic effects. Limited number of literature has been directed toward the biophysical and structural understanding of Hc stability and function. This was not surprising because of the complexity of gastropod Hc structure, created from multiple subunits each containing seven or eight similar, but not identical functional units. As reviewed by Herskovits (1988), the dissociation transitions obtained with the didecameric hemocyanins of land and marine gastropods were considered to be rather complex. The occurrence of didecamer as the predominantly oligomeric form of both KLH1 and KLH2, in in vivo and in vitro conditions, probably relates to the asymmetric nature of the decamer. Till now, no convincingly defined structural difference has been detected between didecamers of KLH1 and KLH2. KLH 1 apparently exists as a stable didecamer with random clusters of didecamers, whereas KLH2 exists as decamers, didecamers, multidecamers of varying length (Gebauer et al. 1994; Sohngen et al. 1997). For KLH2, the production of decamers proved to be slightly more difficult, as simple adjustment of the stabilizing buffer pH had no effect. However, dissociation of KLH2 subunits into a mixture of didecamers and multidecamers was found to be unstable in comparison to that of the KLH1 subunit. It can be concluded that both isoforms of KLH exhibit the characteristics of oligomerization features, whether produced naturally or experimentally. Our experimental results described here allow structural and spectroscopic characterizations of the keyhole limpet hemocyanin from *M. crenulata* (Table 1). Quenching of 'buried tryptophan' by acrylamide explains the structural fluctuation of the protein molecule that facilitates the inward diffusion of the quencher. The lowered K_{sv} values for the KLH at neutral pH in comparison with MG and *N** states reflect the additional limitations of the accessibility to the tryptophyl side chains imposed by the quaternary structure of the aggregates. Two classes of "buried" fluorophores can be considered to be responsible for the Hc fluorescence: first, Trp residues localized very close to the active site pocket; and second, Trp moieties involved in intersubunit contacts (Dolashki et al. 2005). The increase in the quenching

efficiently on the tryptophyl emission can be explained by assuming that upon dissociation, these side chains become more accessible to the quencher, causing the Stern–Volmer constant approach values found for 'exposed' tryptophans as in arthropodan and gastropodan Hcs (Dolashka et al. 1996; Stoeva et al. 1995). As depicted by biophysical techniques, all transition curves for the state at pH 1.2 were found to be similar to that of native KLH. It was reasonable to suggest that in solution the species at pH 1.2 (*N**) resembles KLH at pH 7.4 (*N*). While for the state at pH 2.8 many secondary and tertiary structural elements were found to be preserved, the protein acquires a "globule state". DLS combined with a variety of biophysical methods, such as fluorescence, phase diagram and CD, were used to monitor the changes in conformation and association state of KLH induced at low pH. On the basis of these results, we speculate that our protein contains a mixture of all possible isoforms of Hc (KLH) and that it remains unclear which isoform was responsible for which part of the data. Furthermore, as estimated by the sequence analysis (the KLH sequences were available in the data banks), the pure polypeptides possess 392 kDa; as deduced from sugar analysis, the glycans make another 8–10 kDa. Therefore, it was highly justified to assume a value of ∼8.0 MDa for the KLH didecamer. Our direct measurements of the molecular masses of the two structurally distinct folding intermediates induced by acid, which accumulated at pH 2.8 (decameric, MG state) and 1.2 (tetrameric, *N** state), further approve this hypothesis and clearly support our concept of oligomerization of the KLH subunit. This knowledge would be important for a better understanding of oligomerization of KLH under acidic conditions. In view of the biomedical application of KLH, our results are of particular interest in contributing a series of new physicochemical properties of this complex biopolymer. As shown, KLH didecamers can be quantitatively split into decamers and tetramers at low pH in standard buffer solutions.

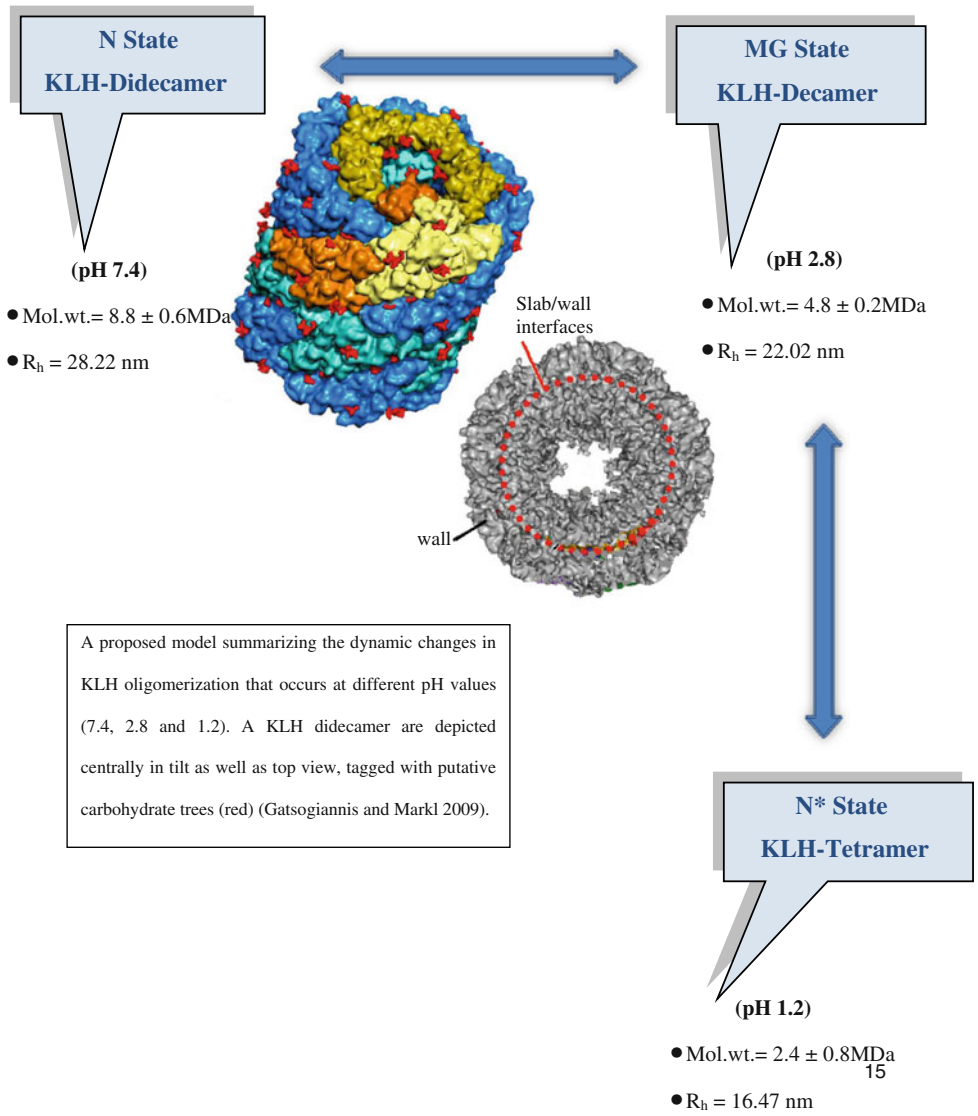

A proposed model summarizing the dynamic changes in KLH oligomerization that occurs at different pH values (7.4, 2.8 and 1.2). A KLH didecamer are depicted centrally in tilt as well as top view, tagged with putative carbohydrate trees (red) (Gatsogiannis and Markl 2009).

Acknowledgments The facilities provided by AMU are gratefully acknowledged. A.V. and B.A. thank the Council of Scientific and Industrial Research, New Delhi, for financial assistance. The authors are also thankful to DST (FIST) for providing laboratory facilities.

References

Ahmad B, Ankita, Khan RH (2005) Urea induced unfolding of F isomer of human serum albumin: a case study using multiple probes. Arch Biochem Biophys 437:159–167

Ahmad B, Ansari MA, Sen P, Khan RH (2006) Low versus high molecular weight polyethylene glycol induced states of stem bromelain at low pH: stabilization of molten globule and unfolded states. Biopolymers 81:350–359

Andrade MA, Chacon P, Merelo JJ, Moran F (1993) Evaluation of secondary structure of proteins from UV circular dichroism spectra using an unsupervised learning neural network. Protein Eng 6:383–390

Beck A, Hillen N, Dolashki A, Stevanovic S, Salvato B, Voelter W, Dolashka-Angelova P (2007) Oligosaccharide structure of a functional unit RvH1-b of *Rapana venosa* hemocyanin using HPLC/electrospray ionization mass spectrometry. Biochimie 89:938–949

Betting DJ, Mu XY, Kafi K, McDonnel D, Rosas F, Gold DP, Timmerman JM (2009) Enhanced immune stimulation by a therapeutic lymphoma tumor antigen vaccine produced in insect cells involves mannose receptor targeting to antigen presenting cells. Vaccine 27:250–259

Bonafe CF, Araujo JRV, Silva JL (1994) Intermediate states of assembly in the dissociation of gastropod hemocyanin by hydrostatic pressure. Biochemistry 33:2651–2660

Chen YH, Yang JT, Martinez H (1972) Determination of the secondary structure of proteins by circular dichroism and optical rotatory dispersion. Biochemistry 11:4120–4131

Cremades N, Sancho J (2008) Molten globule and native state ensemble of *Helicobacter pylori* flavodoxin: can crowding, osmolytes or cofactors stabilize the native conformation relative to the molten globule? Biophys J 95:1913–1927

Decker H, Hellmann N, Jaenicke E, Lieb B, Meissner U, Markl J (2007) Minireview: recent progress in hemocyanin research. Integr Comp Biol 47:631–644

Dolashka P, Genov N, Parvanova K, Voelter W, Geiger M, Stoeva S (1996) *Rapana thomasiana* grosse (gastropoda) haemocyanin: spectroscopic studies of the structure in solution and the conformational stability of the native protein and its structural subunits. Biochem J 315:139–144

Dolashka-Angelova P, Schick M, Stoeva S, Voelter W (2000) Isolation and partial characterization of the N-terminal functional unit of subunit RtH1 from *Rapana thomasiana* grosse hemocyanin. Int J Biochem Cell Biol 32:529–538

Dolashka-Angelova P, Schwarz H, Dolashki A, Beltramini M, Salvato B, Schick M, Saeed M, Voelter W (2003) Oligomeric stability of *Rapana venosa* hemocyanin (RvH) and its structural subunits. Biochim Biophys Acta 1646:77–85

Dolashka-Angelova P, Stevanovic S, Dolashki A, Devreese B, Tzvetkova B, Voelter W, Van Beeumen J, Salvato B (2007) A challenging insight on the structural unit 1 of molluscan *Rapana venosa* hemocyanin. Arch Biochem Biophys 459:50–58

Dolashka-Angelova P, Lieb B, Velkova L, Heilen N, Sandra K, Nikolaeva-Glomb L, Dolashki A, Galabov AS, Van Beeumen J, Stevanovic S, Voelter W, Devreese B (2009) Identification of glycosylated sites in *Rapana* hemocyanin by mass spectrometry and gene sequence, and their antiviral effect. Bioconjug Chem 20:1315–1322

Dolashki A, Schutz J, Hristova R, Voelter W, Dolashka P (2005) Spectroscopic properties of non-glycosilated functional unit KLH2-c of keyhole limpet hemocyanin. World J Agric Sci 1:129–136

Dolashki A, Velkova L, Atanasov B, Voelter W, Stevanovic S, Schwarz H, Muro PD, Dolashka-Angelova P (2008) Reversibility and "pH–T phase diagrams" of *Rapana venosa* hemocyanin and its structural subunits. Biochim Biophys Acta 1784:1617–1624

Eftink MR, Ghiron CA (1982) Fluorescence quenching studies with proteins. Anal Biochem 114:199–227

Gatsogiannis C, Markl J (2009) Keyhole limpet hemocyanin: the 9 ÅCryoEM structure and molecular model of the KLH1 didecamer reveal the interfaces and intricate topology of 160 functional units. J Mol Biol 385:963–983

Gebauer W, Harris JR, Heid H, Sueling M, Hillenbrand R, Soehngen S, Wegener-Strake A, Markl J (1994) Quaternary structure, subunits and domain patterns of two discrete forms of keyhole limpet hemocyanin: KLH1 and KLH2. Zoology 98:51–68

Gebauer W, Stoeva S, Voelter W, Dainese E, Salvato B, Beltramini M, Markl J (1999a) Hemocyanin subunit organization of the gastropod *Rapana thomasiana*. Arch Biochem Biophys 372:128–134

Gebauer W, Harris JR, Geisthardt G, Markl J (1999b) Keyhole limpet hemocyanin type 2 (KLH2): detection and immunolocalization of a labile functional unit h. J Struct Biol 128:280–286

Gebauer W, Harris JR, Markl J (2002) Topology of the 10 subunits within the decamer of KLH, the hemocyanin of the marine gastropod *Megathura crenulata*. J Struct Biol 139:153–159

Georgieva ER, Narvaez AJ, Hedin N, Graslund A (2008) Secondary structure conversions of *Mycobacterium tuberculosis* ribonucleotide reductase protein R2 under varying pH and temperature conditions. Biophys Chem 137:43–48

Gerber R, Tahiri-Alaoui A, Hore PJ, James W (2007) Oligomerization of the human prion protein proceeds via a molten globule intermediate. J Biol Chem 282:6300–6337

Gerber R, Tahiri-Alaoui A, Hore PJ, James W (2008) Conformational pH dependence of intermediate states during oligomerization of the human prion protein. Protein Sci 17:537–544

Geyer H, Wuhrer M, Resemann A, Geyer R (2005) Identification and characterization of keyhole limpet hemocyanin N-glycans mediating cross-reactivity with *Schistosoma mansoni*. J Biol Chem 280:40731–40748

Greene LH, Wijesinha-Bettoni R, Redfield C (2006) Characterization of the molten globule of human serum retinol-binding protein using NMR spectroscopy. Biochemistry 45:9475–9484

Guzman-Casado M, Parody-Morreale A, Mateo PL, Sanchez-Ruiz JM (1990) Differential scanning calorimetry of lobster haemocyanin. Eur J Biochem 188:181–185

Harris JR, Markl J (1999) Keyhole limpet hemocyanin (KLH): a biomedical review. Micron 30:597–623

Harris JR, Markl J (2000) Keyhole limpet hemocyanin: molecular structure of a potent marine immunoactivator: a review. Euro Urol 37(suppl 3):24–33

Harris JR, Gebauer W, Adrian M, Markl J (1998) Keyhole limpet hemocyanin (KLH): slow in vitro reassociation of KLH1 and KLH2 from Immucothel. Micron 5:329–339

Harris JR, Scheffler D, Gebauer W, Lehnert R, Markl J (2000) *Haliotis tuberculata* hemocyanin (HtH): analysis of oligomeric stability of HtH1 and HtH2 and comparison with keyhole limpet hemocyanin KLH1 and KLH2. Micron 31:613–622

Hartmann H, Bongers A, Decker H (2004) Small-angle X-ray scattering based three-dimensional reconstruction of the immunogen KLH1 reveals different oxygen-dependent conformations. J Biol Chem 279:2841–2845

Herskovits TT (1988) Recent aspects of the subunit organization and dissociation of hemocyanins. Comp Biochem Physiol B 91:597–611

Hristova R, Dolashki A, Voelter W, Stevanovic S, Dolashka-Angelova P (2008) *O*-Diphenol oxidase activity of molluscan hemocyanins. Comp Biochem Phys Part B 149:439–446

Ioannes PD, Moltedo B, Oliva H, Pacheco R, Faunes F, Ioannes AED, Becker MI (2004) Hemocyanin of the Molluscan *Concholepas concholepas* exhibits an unusual heterodecameric array of subunits. J Biol Chem 279:26134–26142

Kather I, Jakob RP, Dobbek H, Schmid FX (2008) Increased folding stability of TEM-1 beta-lactamase by in vitro selection. J Mol Biol 383:238–251

Keller H, Lieb B, Altenhein B, Gebauer D, Richter S, Stricker S, Markl J (1999) Abalone (*Haliotis tuberculata*) hemocyanin type 1 (HtH1). Organization of the approximately 400 kDa subunit, and amino acid sequence of its functional units f, g and h. Eur J Biochem 264:27–38

Kim JH, Lee Y, Bae YS, Kim WS, Kim K, Im HY, Kang WK, Park K, Choi HY, Lee HM, Baek SY, Lee H, Doh H, Kim BM, Kim CY, Jeon C, Jung CW (2007) Phase I/II study of immunotherapy using autologous tumor lysate-pulsed dendritic cells in patients with metastatic renal cell carcinoma. Clin Immunol 125:257–267

Kuznetsova IM, Turoverov KK, Uversky VN (2003) Use of the phase diagram method to analyze the protein unfolding–refolding reactions: fishing out the "Invisible" intermediates. J Proteome Res 3:485–494

Lieb B, Markl J (2004) Evolution of molluscan hemocyanins as deduced from DNA sequencing. Micron 35:117–119

Lieb B, Altenhein B, Lehnert R, Gebauer W, Markl J (1999) Subunit organization of the abalone *Haliotis tuberculata* hemocyanin type 2 (HtH2), and the cDNA sequence encoding its functional units d, e, f, g and h. Eur J Biochem 265:134–144

Lieb B, Altenhein B, Markl J (2000) The sequence of a gastropod hemocyanin (HtH1 from *Haliotis tuberculata*). J Biol Chem 275:5675–5681

Lieb B, Altenhein B, Markl J, Vincent A, Van Olden EV, Van Holde KE, Miller K (2001) Structures of two molluscan hemocyanin genes: significance for gene evolution. Proc Natl Acad Sci USA 98:4546–4551

Lowry OH, Rosebrough NJ, Farr AL, Randall RJ (1951) Protein measurement with the folin–phenol reagent. J Biol Chem 193:265–275

Markl J, Savel-Niemann A, Wegener-Strake A, Sueling M, Schneider A, Gebauer W, Harris JR (1991) The role of two distinct subunit types in the architecture of keyhole limpet hemocyanin (KLH). Naturwissenschaften 78:512–514

Martin A, Depoix F, Stohr M, Meissner U, Hagner-Holler S, Hammouti K, Burmester T, Heyd J, Wriggers W, Markl J (2007) *Limulus polyphemus* hemocyanin: 10 Å structure, sequence analysis, molecular modelling and rigid-body fitting reveal the interfaces between the eight hexamers. J Mol Biol 366:1332–1350

Mouche F, Zhu YX, Pulokas J, Potter CS, Carragher B (2003) Automated three-dimensional reconstruction of keyhole limpet hemocyanin type 1. J Struct Biol 144:301–312

Nishimura C, Dyson HJ, Wright PE (2008) The kinetic and equilibrium molten globule intermediates of apoleghemoglobin differ in structure. J Mol Biol 378:715–725

Orlova EV, Dube P, Harris JR, Beckman E, Zemlin F, Markl J, van Heel M (1997) Structure of keyhole limpet hemocyanin type 1 (KLH1) at 15 Å resolution by electron cryomicroscopy and angular reconstitution. J Mol Biol 271:417–437

Paci E, Greece LH, Jones RM, Smith LJ (2005) Characterization of the molten globule state of retinol-binding protein using a molecular dynamics simulation approach. FEBS J 18:4826–4838

Pawar SA, Deshpande VV (2000) Characterization of acid-induced unfolding intermediates of glucose/xylose isomerase. Eur J Biochem 267:6331–6338

Ramboarina S, Redfield C (2008) Probing the effect of temperature on the backbone dynamics of the human α-lactalbumin molten globule. J Am Chem Soc 130:15318–15326

Riggs DR, Jackson B, Vona-Davis L, McFadden D (2002) In vitro anticancer effects of a novel immunostimulant: keyhole limpet hemocyanin. J Surg Res 108:279–284

Sabbatini PJ, Ragupathi G, Hood C, Aghajanian CA, Juretzka M, Iasonos A, Hensley ML, Spassova MK, Ouerfelli O, Spriggs DR, Tew WP, Konner J, Clausen H, Abu Rustum N, Dansihefsky SJ, Livingston PO (2007) Pilot study of a heptavalent vaccine—keyhole limpet hemocyanin conjugate plus QS21 in patients with epithelial ovarian, fallopian tube, or peritoneal cancer. Clin Cancer Res 13:4170–4177

Sandra K, Dolashka-Angelova P, Devreese B, Van Beeumen J (2007) New insights in *Rapana venosa* hemocyanin N-glycosylation resulting from on-line mass spectrometric analyses. Glycobiology 17:141–156

Semisotnov GV, Rodionova NA, Razgulyaev OI, Uversky VN, Gripas AF, Gilmanshin RI (1991) Study of the "molten globule" intermediate state in protein folding by a hydrophobic fluorescent probe. Biopolymers 1:119–128

Sohngen MS, Stahalmann A, Harris JR, Muller SA, Engel A, Markl J (1997) Mass determination, subunit organization and control of oligomerization states of keyhole limpet hemocyanin (KLH). Euro J Biochem 248:602–614

Sterner R, Decker H (1994) Inversion of the Bohr effect upon oxygen binding to 24-meric *tarantula* hemocyanin. Proc Natl Acad Sci USA 91:4835–4839

Stoeva S, Dolashka P, Bankov B, Voelter W, Salvato B, Genov N (1995) Spectroscopic properties of *Callinectes sapidus* hemocyanin subunits. Spectrochim Acta 51A:1965–1974

Suminoe A, Matsuzaki A, Hattori H, Koga Y, Hara T (2008) Immunotherapy with autologous dendritic cells and tumor antigens for children with refractory malignant solid tumors. Pediatr Transpl 13:746–753

Van Holde KE, Miller KI (1995) Hemocyanins. Adv Protein Chem 47:1–81

Van Holde KE, Miller KI, Lang WH (1992) Molluscan hemocyanins: structure and function. Adv Comp Environ Physiol 13:257–300

Varshney A, Ahmad B, Khan RH (2008) Comparative studies of unfolding and binding of ligands to human serum albumin in the presence of fatty acid: spectroscopic approach. Int J Biol Macromol 42:483–490

Velkova L, Dolashka-Angelova P, Dolashki A, Voelter W, Atanasov B (2009) Thermodynamic analysis and molecular modeling of *Rapana venosa* hemocyanin—functional unit RVH2-E. Biotechnol Biotechnol Eq 23:601–605

Yang F Jr, Zhang M, Chen J, Liang Y (2006) Structural changes of alpha-lactalbumin induced by low pH and oleic acid. Biochim Biophys Acta 1764:1389–1396